SUPPLEMENTS

Supplementary Table 1. Summary of quantitative results from human studies using HP ^{13}C-MRI

Authors*	Clinical applications	Quantitative results	Additional results
Brain			
Miloushev et al., 2018 [25]	1st human brain tumor study	*Kinetic modeling* Whole brain: k_{PL} = 0.12	Higher production of Pyr and Lac in normal cortical/subcortical regions; glycolytic heterogeneity among different brain tumors
Autry et al., 2020 [26]	Post radio-chemotherapy follow-up in infiltrative glioma	*Kinetic modeling* Glioma patient Normal brain: k_{PL} = 0.020, k_{PB} = 0.006; normal brain post bevacizumab: k_{PL} = 0.047, k_{PB} = 0.011; glioma (contrast enhancing): k_{PL} = 0.032–0.041; glioma (T2 hyperintense): k_{PL} = 0.024 Healthy volunteer Normal brain: k_{PL} = 0.018, k_{PB} = 0.004	Global elevation of k_{PL} and k_{PB} post bevacizumab; elevated k_{PL} and k_{PB} in progressive disease
Autry et al., 2021 [27]	Pediatric brain tumor vs. normal brain, pediatric safety profile	*Model free* Whole brain: SNR_{Pyr} = 7.85 x 10^2–3.52 x 10^5, SNR_{Lac} = 1.75 x 10^2–7.20 x 10^4, SNR_{Bic} = 64–1.52 x 10^4	Safety of HP ^{13}C-MRI in pediatric patients
Lee et al., 2021 [28]	Prediction of radiotherapy response in intracranial metastases	*Model free* z-score = -2.33–3.74	Tumors with highest z-scores are associated with radiotherapy failure
Chen et al., 2021 [29]	Glioblastoma vs. normal brain	*Model free* Glioblastoma: Lac/TC = 0.310, Bic/TC = 0.086; normal brain: Lac/TC = 0.246, Bic/TC = 0.108	1st vs. 2nd injections: metabolites/TC were insignificantly higher in 2nd injection
Zaccagna et al., 2022 [30]	Glioblastoma vs. normal brain	*Kinetic modeling* (x10^{-3}) Glioblastoma: k_{PL} = 16.1, k_{PB} = 1.7; normal brain: k_{PL} = 16.5, k_{PB} = 2.4 *Model free* Glioblastoma: Lac/Pyr = 0.34, Bic/Pyr = 0.06; normal brain: Lac/Pyr = 0.36, Bic/Pyr = 0.10	Bic/Pyr negatively correlates with lesion volume and volume of enhancing tissue; Bic/Pyr positively correlates with percentage of non-enhancing core; LDHA positively correlates with Lac/Pyr; MCT4 positively correlates with Bic/Pyr and Bic/Lac
Grist et al., 2019 [31]	Technical feasibility in healthy human brain	*Kinetic modeling* Whole brain: k_{PL} = 0.012, k_{PB} = 0.002	Higher metabolites signal in gray matter compared to white matter
Lee et al., 2020 [32]	Metabolite topography in healthy human brain	Not available	Lac topography unveils a region-specific distribution of Lac in the brain, which is consistent across individuals
Hackett et al., 2020 [33]	Traumatic brain injury	*Model free* Patient 1: trauma vs normal: Bic/TC = 0.027 vs. 0.059, Lac/TC = 0.236 vs. 0.191 Patient 2: trauma vs normal: Bic/TC = 0.025 vs. 0.047, Lac/TC = 0.164 vs. 0.162	Mild traumatic brain injury without discernible anatomic change or hemorrhage on MRI
Ma et al., 2022 [34]	Technical feasibility in healthy human brain	*Kinetic modeling* Whole brain: k_{PL} = 0.014–0.018, k_{PB} = 0.004–0.006 *Model free* Whole brain: Lac/TC = 0.21–0.24, Bic/TC = 0.065–0.091	Lac/TC and Bic/TC linearly correlate with fractional gray matter volume
Uthayakumar et al., 2023 [35]	Metabolic changes in brain aging	*Model free* A 7% ± 2% decrease per decade for Lac and a 9% ± 4% decrease per decade for Bic	Variability in aging-related metabolic changes is observed across different brain regions
Heart and skeletal muscle			
Cunningham et al., 2016 [36]	1st human healthy heart study	*Model free* SNR_{Pyr} = 115, SNR_{Bic} = 56, SNR_{Lac} = 53	Pyr signal observed only in cardiac chamber, Bic only in myocardium, Lac in both chamber and myocardium
Rider et al., 2020 [37]	Healthy vs. diabetic heart	*Model free* (x 10^{-2}) Healthy heart: Bic/Pyr = 0.84, Lac/Pyr = 5.16, Ala/Pyr = 3.17; diabetic heart: Bic/Pyr = 0.16, Lac/Pyr = 8.51, Ala/Pyr = 3.82	Significantly increased Pyr-to-Bic flux after oral glucose challenge
Park et al., 2020 [38]	Cardiotoxicity of doxorubicin	*Model free* Before doxorubicin: Bic/TC = 0.036, Lac/TC = 0.448, Ala/TC = 0.045; after doxorubicin: Bic/TC = 0.032, Lac/TC = 0.440, Ala/TC = 0.045	Hemoglobin, high-sensitivity troponin, and left ventricular global longitudinal strain also change after chemotherapy
Ma et al., 2022 [39]	End diastolic vs. end systolic in healthy heart	*Model free* End diastolic to end systolic: Bic/Lac = 21.6 decrease, Bic/Ala = 9.4 decrease	The decrease in Bic/Lac from end diastolic to end systolic occurs prominently in the mid-anterior and mid-inferoseptal segments of heart
Park et al., 2021 [40]	Rest vs. exercise vs. recovery in healthy calf skeletal muscle	*Model free* Rest: Lac/TC = 0.18, Bic/TC = 0.004; exercise: Lac/TC = 0.31, Bic/TC = 0.036; recovery: Lac/TC = 0.42, Bic/TC = 0.002	TC (perfusion) at rest increases to 2.8-fold with exercise and to 3.2-fold during recovery
Body and oncology			
Woitek et al., 2020 [41]	Post neoadjuvant chemotherapy follow-up in breast cancer	*Kinetic modeling* 37% decrease in k_{PL} after neoadjuvant chemotherapy *Model free* 34% decrease in Lac/Pyr after neoadjuvant chemotherapy	After neoadjuvant chemotherapy 76% decrease in tumor volume but 132% increase in K^{trans} and 31% increase in k_{ep}; pathologic complete response after neoadjuvant chemotherapy
Woitek et al., 2021 [42]	Very early neoadjuvant chemotherapy response assessment in breast cancer	*Kinetic modeling* Breast cancer post chemotherapy k_{PL} = 0.0064 → 0.0079 *Model free* Breast cancer post chemotherapy: SNR_{Pyr} = 19.7 → 16.5, SNR_{Lac} = 7.0 → 4.5, Lac/Pyr = 0.28 → 0.34	≥ 20% increase of Lac/Pyr predicts pathologic complete response
Tran et al., 2019 [43]	Intratumoral metabolic heterogeneity of RCC	Not available	Variability in Lac signal correlates with Lac levels in tumor samples on LC-MS analysis
Tang et al., 2021 [44]	Tumor grade and histopathologic type of RCC	*Model free* Lac/Pyr: chromophobe RCC > grade 3 ccRCC > grade 2 ccRCC	Demonstration of good reproducibility of HP ^{13}C-MRI by performing 2 acquisitions in the same day
Ursprung et al., 2022 [45]	Prediction of tumor grade of RCC	*Kinetic modeling* (median) k_{PL}: ccRCC = 0.0065, normal kidney = 0.0043, liposarcoma = 0.0152, pheochromocytoma = 0.0086, oncocytoma = 0.0022 *Model free* (median) SNR_{Pyr}: ccRCC = 26.7, normal kidney = 30.1, liposarcoma = 31.9, pheochromocytoma = 34.0, oncocytoma = 12.3; SNR_{Lac}: ccRCC = 5.7, normal kidney = 3.4, liposarcoma = 10.5, pheochromocytoma = 6.0, oncocytoma = 1.0; Lac/Pyr: ccRCC = 0.13, normal kidney = 0.14, liposarcoma = 0.35, pheochromocytoma = 0.17, oncocytoma = 0.14	Increasing k_{PL} correlates with higher tumor grade; Lac/Pyr negatively correlates with ADC; MCT1 expression (but not MCT4) positively correlates with k_{PL}; MCT1 expression independently predicts overall survival of RCC patients
Lee et al., 2022 [46]	Comparison among normal intrabdominal solid organs: liver, kidney, pancreas, spleen	*Kinetic modeling* k_{PL}: liver = 0.019, kidney (R) = 0.0036, kidney (L) = 0.0033, pancreas = 0.0063, spleen = 0.0096; k_{PA}: liver = 0.012, kidney (R) = 0.0011, kidney (L) = 0.00087, pancreas = 0.0034, spleen = 0.00073	The liver exhibits a comparatively lower absolute metabolite signal, yet the highest metabolite conversion rates
Stødkilde-Jørgensen et al., 2020 [47]	Tumor vs. normal in pancreatic cancer	*Model free* Pancreatic cancer: Ala/Lac = 0.33; normal pancreas: Ala/Lac = 0.23	Ala/Lac as a potential biomarker to detect pancreatic ancer
Gordon et al., 2023 [48]	Tumor vs. normal, early response prediction in pancreatic cancer	*Model free* Pancreatic cancer: Lac/Pyr = 0.30–1.65, Ala/Pyr = < 0.01–0.14, Ala/Lac = < 0.01–0.46; normal pancreas: Lac/Pyr = 0.20–0.27, Ala/Pyr = 0.06–0.15, Ala/Lac = 0.24–0.79	Early metabolic response at 4 weeks correlates with subsequent tumor response
Nelson et al., 2013 [49]	Tumor vs. normal in prostate cancer	*Kinetic modeling* Prostate cancer: k_{PL} = 0.013	1st human study in prostate cancer, safety profile
Aggarwal et al., 2017 [50]	Early response for androgen deprivation therapy in prostate cancer	*Kinetic modeling* Prostate cancer post androgen deprivation therapy: k_{PL} = 0.025 → 0.007	Only modest changes in tumor size and ADC value
Chen et al., 2020 [51]	Feasibility in bone and liver metastasis in castration-resistant prostate cancer	*Kinetic modeling* Bone metastases: k_{PL} = 0.020; liver metastases: k_{PL} = 0.026; liver metastasis post chemotherapy: k_{PL} = 0.026 → 0.015 *Model free* Bone metastasis: SNR_{TC} = 117; liver metastasis: SNR_{TC} = 85	RNA-seq found higher LDHA expression relative to the dominant isoform of LDH
Granlund et al., 2020 [52]	Tumor grade of prostate cancer	*Model free* max Lac/TC = 0.35 Time to max Lac/TC = 44 s	Lac increases with Gleason tumor grade; regions exhibiting high Lac also show high MCT1 expression and loss of PTEN
de Kouchkovsky et al., 2022 [53]	Early immunotherapy response assessment in castration-resistant prostate cancer	*Kinetic modeling* Prostate cancer post immunotherapy: k_{PL} = 0.0273 → undetectable, k_{PL} = 0.0147 → 0.0006	Metabolic response is more significant than morphologic response
Chen et al., 2022 [54]	Integration with MR/TRUS fusion-guided biopsy in prostate cancer	*Kinetic modeling* k_{PL} > 0.02 as biomarker of suspected cancer; prostate cancer: k_{PL} = 0.0319; normal prostate: k_{PL} = 0.0110	4 of 6 k_{PL} targets on HP ^{13}C-MRI did not correlate to PIRDAS targets on conventional MRI
Sushentsev et al., 2022 [55]	Metabolic phenotyping in intermediate risk prostate cancer	*Kinetic modeling* Prostate cancer: k_{PL} = 0.011 *Model free* Prostate cancer: SNR_{Lac} = 12, SNR_{Pyr} = 33, SNR_{TC} = 53	SNR_{Lac} positively correlates to % Gleason pattern 4 and mean ADC values
Lin et al., 2024 [56]	Immune activation of spleen post chemoradiotherapy	*Model free* (x 10^{-2}) Responder: Pyr/TC = 91.5, Lac/TC = 3.6; nonresponder: Pyr/TC = 74.4, Lac/TC = 19.9	Lower baseline metabolism in spleen correlates with better response to chemoradiotherapy

Unless specified otherwise, data are presented as mean values.
*The numbers enclosed in brackets correspond to the numbers of the articles listed in the reference section of the main paper.
HP = hyperpolarized, Pyr = pyruvate, Lac = lactate, Ala = alanine, Bic = bicarbonate, TC = total carbon, SNR = signal-to-noise ratio, LDH = lactate dehydrogenase (isoform: LDHA), MCT = monocarboxylate transporter (isoform: MCT1, MCT4), RCC = renal cell carcinoma, cc = clear cell, ADC = apparent diffusion coefficient, TRUS = transrectal ultrasound

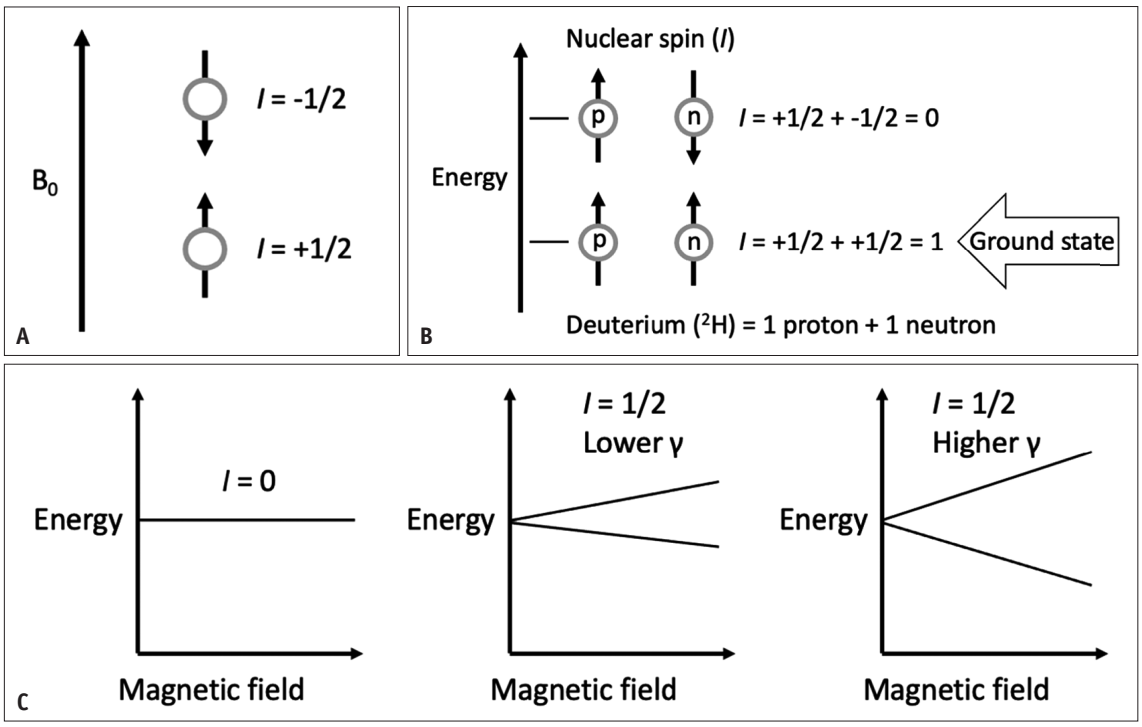

Supplementary Fig. 1. Fundamental principles of nuclear spin. **A:** Nuclear spin is an intrinsic property of particles, always manifesting as either +1/2 or -1/2. **B:** In nature, nuclear spin results from the combined spins of protons and neutrons, existing exclusively in the ground state (I) with values such as 0, 1/2, 1, 3/2, and so on. **C:** The ground state comprises "$2I + 1$" sublevels. Upon the application of a magnetic field, slight energy differences arise between these sublevels, leading to Zeeman splitting. Nuclei with $I = 0$ exhibit only one sublevel, lack Zeeman splitting, and remain inactive in MRI (^{12}C), whereas nuclei with $I \neq 0$ (^{1}H and ^{13}C) are nuclear magnetic resonance active due to having multiple sublevels. Notably, nuclei with higher gyromagnetic ratios (γ) experience more significant splitting when a magnetic field is applied.

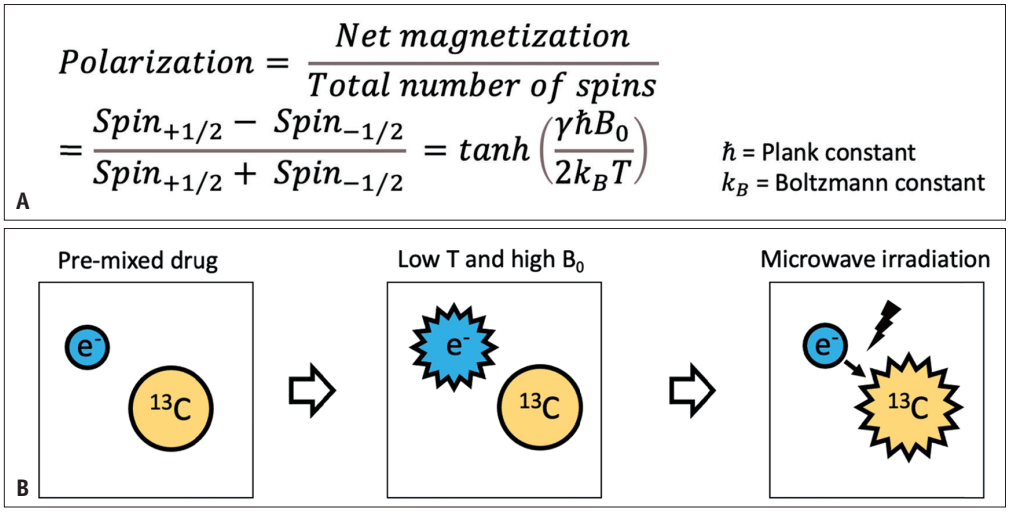

Supplementary Fig. 2. Basic concepts of DNP. **A:** Polarization is a function of gyromagnetic ration (γ), magnitude of magnetic field (B_0), and temperature (T). To polarize nuclei with lower γ, higher magnetic field and lower temperature environment are required. For example, clinical polarizer SPINlab™ operates at B_0 = 5T and T = 0.8 k. **B:** Directly polarizing the ^{13}C nucleus (the brute force method) presents an engineering challenge and is time-consuming, making it impractical for clinical use. Electrons have a high γ of 28025 and are more amenable to polarization. DNP offers a clinically feasible solution by transferring polarization from electrons to ^{13}C nuclei, achieving 20%–30% ^{13}C polarization (equivalent to > 10000 signal enhancement) within 2–3 hours. DNP = dynamic nuclear polarization